

Szymon SOBCZYK, Leszek MIKULSKI

KRAKOW UNIVERSITY OF TECHNOLOGY, INSTITUTE OF BUILDING MECHANICS
DEPARTMENT OF THE FUNDAMENTALS OF THE MECHANICS OF CONTINUOUS MEDIA
Warszawska St. 24, Krakow, Poland

A method of optimum selection of post-tensioned concrete beam prestressing by example of a symmetrical three-span beam

Abstract

The article presents an original optimisation method developed by authors, which combines the method of simple gradient and iterative solution to an optimisation problem formulated. The innovative design method is presented by example of forming a symmetrical three-span post-tensioned concrete beam. The mathematical notation of the routes of prestressing tendons is presented along with the iterative algorithm, which allows for finding quickly an optimum solution to the optimisation problem in question. Based on the results of calculations performed, recommendations are given for the prestressing tendons routing in symmetrical three-beam post-tensioned concrete beams.

Keywords: structure optimisation, post-tensioned concrete beams, resultant route of prestressing tendons.

1. Introduction

In the contemporary design of construction components, the economic aspects of the solutions applied are in the centre of attention. Therefore, the computational methods for resolving the optimisation issues are becoming increasingly important. In an economic design, the cost related to the construction of a specific component in the project concerned has to be analysed in detail before the calculations are made. Not in every single case will an optimum component imply the minimum use of materials. Every contractor is able to determine cost-effective proportions to minimise the overall cost of fabrication of a specific component.

While designing post-tensioned concrete components with the modern engineering methods and based on the popular literature of the subject [1, 2, 3, 4, 5], it is particularly difficult to simultaneously analyse the effect of the multiple decision variables on the solution possible. The main reason for that is the absence of specialised software for modelling the routes of prestressing tendons and determining the prestressing force acting on the structure. Without the use of advanced software, the effect of prestressing on a structure can be determined, among others, with the method of substitute effects [3, 4] or using the line of influence [5].

In statically indeterminate systems, the prestressing force causes additional reactions to occur in the supporting bonds, which are the effect of the structure constriction. A secondary effect of the supporting bond reactions are the excited forces, i.e. such additional inner forces which cannot be calculated only from the tendon geometry in relation to the axis of sectional inertia. When the excited force values are low, the concurrent tendon route is the case, i.e. when the inner forces do not depend on the static diagram of the structure. Therefore, the concurrent route can be set as the design objective to enable designing of components without detailed calculations of the effects of prestressing which considerably streamlines the design task. For that reason, the concurrent tendon routes are very often sought in the contemporary design of post-tensioned concrete components. The methods for finding them are broadly discussed in [1, 3, 5]. However, note that the deviation from the concurrent route often allows the redistribution of the inner forces into the desired intended structure area.

2. Calculation methods

The gradient iterative optimisation method being developed at the Krakow University of Technology, Institute of Building Mechanics was used for the study [9, 10]. The method combines

a simple gradient method and iterative solution to the formulated optimisation problem. In general, the application of the method can be described in 6 steps:

1. Mathematical notation of functions describing the optimisation task in question.
2. Determination of the objective function and decision variables.
3. Determination of optimisation restrictions.
4. Determination of optimisation starting point and directions to seek the solution.
5. Description of the incremental function.
6. Iterative finding of a solution meeting the optimisation criteria set.

The method described can be applied in solving various optimisation problems. An optimum solution can be found with the aid of common software in incomparably less time than in the case of optimisation with other methods.

Combined with the finite element method, this method enables very quick solving of optimisation problems of statically indeterminate structures.

While formulating a task for the gradient iterative method, simple functions are applied which make it possible to describe the optimisation problem being considered. The functions determined are introduced in computational loops. Numerical calculations are performed very fast thanks to the simple mathematical notation.

While describing a specific issue, particular attention should be brought to the proper determination of the incremental function. Otherwise, the calculation time can be significantly extended or, in the worst scenario, it can be impossible to achieve a reliable result.

Static analysis of flat bent bar systems is among the typical problems of the structure mechanics [6, 7, 8]. Linear rigidity matrices of bars, geometrical rigidity and consistent weight matrices are found based on which finite element method (FEM) software is developed. The FEM issues for bar systems are not covered in this article.

2.1. Decision variables

Five decision variables were specified for the optimisation task:

- Z1. Cross-sectional height.
- Z2. Tendon route with any trajectory.
- Z3. Prestressing force N .
- Z4. Prestressing force N_1 .
- Z5. Prestressing force N_2 .

The optimisation task analysed is of a multiple-decision nature, since in design practice it is rarely a single variable that determines the optimality (in terms of cost-effectiveness) of a given solution.

2.2. Inner forces from prestressing

The task involves optimisation of a three-span post-tensioned concrete beam. For the system being statically indeterminate, the compression force induce hyperstatic forces.

Since the problem in question involves a continuous beam with any prestressing method, three possible routes of the resultant tendons were determined:

- N - resultant tendon with any trajectory;

- N_1 - resultant tendon with a linear trajectory, at the lower section edge;
- N_2 - resultant tendon with a linear trajectory, at the upper section edge.

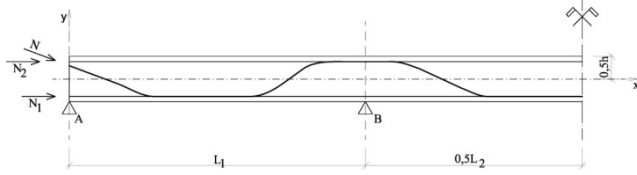


Fig. 1. Prestressing tendon route

The effects of tendons on the structures is broadly described, inter alia in [4, 5]. In the study, the method of equivalent loads was applied to determine the inner forces resulting from prestressing in a statically indeterminate system.

To determine the excited forces caused by the prestressing forces in the beam, a substitute system of forces was adopted that induces equivalent hyperstatic reactions.

In the algorithm, the considerations were limited to the case of a three-span beam which was divided to 12 calculation points arranged according to the points of inflection of the prestressing tendon route N . Sections 1-2, 3-4, 5-6, 7-8, 9-10, 11-12 are straight, and the fragments 2-3, 4-5, 6-7, 8-9, 10-11 are curvilinear (Fig. 2).

The prestressing forces N , N_1 , N_2 were substituted with the system shown in Figure 2. The system comprises:

- the shear force $N\sin(\alpha_1)$;
- the compressive force N_s ;
- the bending moment M ;
- the continuous load q_{si} located at curvilinear sections of the prestressing tendon N (the force is created as a result of the route curvature change at bends).

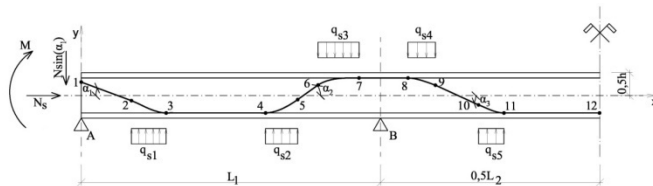


Fig. 2. Substitute loads

The total prestressing force value is described with the equation:

$$N_s = N\cos(\alpha_1) + N_1 + N_2 \quad (1)$$

While the bending moment M :

$$M = N\cos(\alpha_1)e + N_1e_1 + N_2e_2 \quad (2)$$

The forces q_{si} were determined from the dependencies:

$$q_{s1} = \frac{N\sin(\alpha_1)}{x_3 - x_2} \quad (3)$$

$$q_{s2} = \frac{N\sin(\alpha_2)}{x_5 - x_4} \quad (4)$$

$$q_{s3} = \frac{N\sin(\alpha_2)}{x_7 - x_6} \quad (5)$$

$$q_{s4} = \frac{N\sin(\alpha_3)}{x_9 - x_8} \quad (6)$$

$$q_{s5} = \frac{N\sin(\alpha_3)}{x_{11} - x_{10}} \quad (7)$$

where:

x_i - coordinate x of the i^{th} calculation point;

α_i - inclination angles between the points of inflection of the tendon route.

2.3. Mathematical notation of the prestressing tendon

In order to create an optimising function, the resultant tendon route was divided into 12 calculation points. For each point, the coordinates X_j and Y_j were determined. For the technical possibility of routing the prestressing tendons, it was assumed that:

- sections 1-2, 3-4, 5-6, 7-8, 9-10, 11-12 are straight,
- while fragments 2-3, 4-5, 6-7, 8-9, 10-11 are curvilinear.

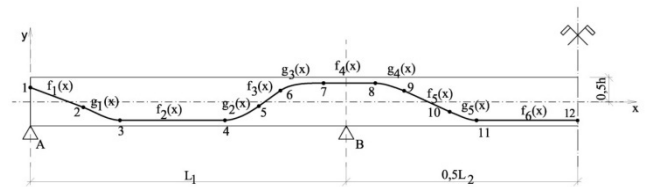


Fig. 3. Characteristic points of the tendon route and function determination

A spline was created between the characteristic points. Since the tendon has to be routed without sharp turns, the convergence of tangents of the adjacent sections was assumed. In the solution, overlapping of the characteristic points for straight sections is allowed. This assumption allows generating a spline composed only of curvilinear sections.

In order to generate the spline, at first, the direction factors a_i and other free terms b_i are determined for the linear functions by means of the function:

$$a_i = \text{slope} \left[\left(X_j, Y_j \right), \left(X_{j+1}, Y_{j+1} \right) \right] \quad (8)$$

$$b_i = \text{intercept} \left[\left(X_j, Y_j \right), \left(X_{j+1}, Y_{j+1} \right) \right] \quad (9)$$

where:

slope - function that returns the direction factor for the linear function between points j and $(j+1)$;

intercept - function that returns the free term for the linear function between points j and $(j+1)$.

Based on the factors a_i and b_i established, the linear functions are determined:

$$f_i(x) = a_i x + b_i \quad (10)$$

To determine curvilinear sections, the 3rd order regression function was applied, placed between the characteristic points and the points located near the characteristic point outside the curvilinear section being determined. To match the shape of the spline precisely, the points to be used for regression were assumed to be at the distance $\Delta = 0.05$ m (Fig. 4).

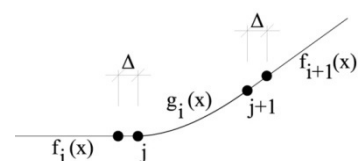


Fig. 4. Curvilinear sections with the surroundings

The curvilinear function was determined with the formula:

$$g_i(x) = \begin{cases} vs \leftarrow regress \left[\begin{pmatrix} X_j - \Delta \\ X_j \\ X_{j+1} \\ X_{j+1} + \Delta \end{pmatrix}, \begin{pmatrix} f_i(X_j - \Delta) \\ Y_j \\ Y_{j+1} \\ f_{i+1}(X_{j+1} + \Delta) \end{pmatrix} \right], k \\ interp \left[vs, \begin{pmatrix} X_j - \Delta \\ X_j \\ X_{j+1} \\ X_{j+1} + \Delta \end{pmatrix}, \begin{pmatrix} f_i(X_j - \Delta) \\ Y_j \\ Y_{j+1} \\ f_{i+1}(X_{j+1} + \Delta) \end{pmatrix} \right], x \end{cases} \quad (11)$$

where:

- k - positive integer denoting the regression order;
- regress* - function that returns the vector used by the function *interp*;
- interp* - function that returns the k -th order polynomial that best approximates the specified data set.

Ultimately, the spline takes the form:

$$h(x) = \begin{cases} f_1(x) & \text{if } X_1 \leq x < X_2 \\ g_1(x) & \text{if } X_2 \leq x < X_3 \\ f_2(x) & \text{if } X_3 \leq x < X_4 \\ g_2(x) & \text{if } X_4 \leq x < X_5 \\ f_3(x) & \text{if } X_5 \leq x < X_6 \\ g_3(x) & \text{if } X_6 \leq x < X_7 \\ f_4(x) & \text{if } X_7 \leq x < X_8 \\ g_4(x) & \text{if } X_8 \leq x < X_9 \\ f_5(x) & \text{if } X_9 \leq x < X_{10} \\ g_5(x) & \text{if } X_{10} \leq x < X_{11} \\ f_6(x) & \text{if } X_{11} \leq x < X_{12} \end{cases} \quad (11)$$

The above is a notation of the function that reaches to the half of the beam span. The function is symmetrical with respect to point 12.

The coordinates of the characteristic points are determined based on the variability assumed. The table below summarizes the number of possible combinations of the coordinates X depending on the assumed size of the relative change in the position of the characteristic points. Due to the varying number of characteristic points of the first span relative to the second one, the table shows the selected density configurations. For the possible combinations of coordinates, overlapping of the characteristic points of linear sections is allowed. However, this is not allowed for the curvilinear sections. This is due to the fact that the prestressing tendons cannot be routed with sharp points of inflection.

Tab. 1. Possible combination of the coordinates X depending on the assumed density of calculation points.

Division L_1	Division $0.5L_2$	Combinations
7	4	140
8	5	1,260
9	5	3,150
10	6	16,170
11	6	32,340
12	7	120,120
12	8	216,216
13	9	630,630
13	10	990,990
14	10	1,651,650

The table above shows the number of possible positions of the coordinates X depending on the adopted division. It should be noted that the table shows only the possible configurations of the coordinates X . For the entire result base of the coordinates XY , the above values should be multiplied by the number of combinations of the coordinates Y . Given the vast number of the potential resultant tendon routes, fragmentary calculations were performed

with the export to the external resultant databases. It was also assumed to reduce the number of the possible locations of the coordinates X in the first iterations. More accurate results are achieved in the following iterations by gradient change of the location of route point coordinates for which the optimisation criteria have been met.

2.4. Gradient iterative method in the task analysed

Due to the presence of several decision variables, the optimisation task considered was divided into 2 basic stages:

- Preliminary calculations.
- Detailed calculations within a given iteration.

Preliminary calculations

In order to accelerate the calculation process, preliminary calculations are performed before tackling the specific optimisation task, aimed at determining the starting parameters of the optimisation of the boundaries of the decision variables. Calculations for that stage are characterised by considerably lower accuracy which is yet sufficient for an indicative estimation of the expected variability range of the decision parameters. The preliminary calculations used the following:

- height increment $\Delta h = 200$ mm;
- prestressing force increment $\Delta N = 500$ kN;
- variability of location of the characteristic points of the resultant tendon route: $\Delta x = 3$ m.

Detailed calculations within a given iteration

1st iteration

In the optimisation task in question, the objective function was adopted:

- concrete volume:

$$f_c = \int_0^{L_c} A(x) dx \quad (12)$$

where:

$A(x)$ - cross-sectional area.

Calculations of the first iteration are performed for a determined base of the possible prestressing tendon routes with any trajectory.

For each of the routes possible, an optimal value is found of the other decision variables which will minimise the determined objective function. In the next stage, from the resultant set of optimal solutions created for individual tendon routes, solutions are selected for which the best result has been obtained. In the first iteration, due to inaccurate data from the initial calculations, the variability range h, N, N_1 and N_2 is relatively broad and, therefore, it is not recommended to adopt the accuracy exceeding:

- the height increment $\Delta h = 100$ mm;
- the prestressing force increment $\Delta N = 500$ kN.

Furthermore, for the first iteration calculations, for a very large set of possible tendon routes, it is not recommended to divide the inter-span sections to more than 16 finite elements. Increasing the number of finite elements does not considerably improve the accuracy of the optimisation calculations, but makes the operation more time-consuming. Note that the first iteration calculations are intended to eliminate solutions which do not meet the specified optimisation criteria and differ significantly from the expected value of the objective function.

2nd iteration

Having a set of solutions at hand that meets the optimisation criteria established, more accurate calculations are performed. To this end, the finite element lattice is densified and the changeability area of the decision parameters is changed.

Based on the results of the first iteration, starting parameters of the decision variables are determined. For the optimisation case of concrete volume minimisation, it is assumed:

$$h_0^{II} = h_{opt}^I - \Delta h^I \quad (13)$$

where:

h_0^{II} - starting height of the 2nd iteration;
 h_{opt}^I - optimum height determined in the calculations of the first iteration.

Because of the search for a solution that will minimise the concrete volume, the decision variable h increases according to the following formula:

$$h_i^{II} = \begin{cases} \text{while } h_{i-1}^{II} \leq h_{opt}^I \\ h_i^{II} \leftarrow h_{i-1}^{II} + \Delta h^{II} \end{cases} \quad (14)$$

For each variable h , all possible configurations of the prestressing tendon and prestressing forces are analysed. On finding a solution that meets the specific optimisation criteria, the calculations are stopped and discontinued for greater values of the variable h .

Following iterations

In the following iterations, in addition to the aforementioned increase of the decision variable, the gradient location change of the characteristic points of the resultant prestressing tendon is analysed. In calculations, the possible shift is considered in any direction by the value:

$$\Delta x^i = \frac{\Delta x^{i-1}}{n_x} \quad (15)$$

where:

n_x - determined density of the changeability of the resultant tendon location;
 Δx^i - changeability of the resultant tendon location for the i -th iteration;
 Δx^{i-1} - changeability of the resultant tendon location for the $(i-1)$ -th iteration.

Coordinates of the route points are determined as a vector of possible locations, according to the formula:

$$X^i = \begin{cases} \text{for } j \in (-n_x), (-n_x + 1) \dots (n_x - 1), n_x \\ X_j^i \leftarrow X^{i-1} + j \Delta x^i \end{cases} \quad (16)$$

where:

X_j^i - j -th line of the vector of possible locations of the coordinate X in the i -th iteration;
 X^{i-1} - coordinate X in the $(i-1)$ -th iteration.

The calculations are performed until the determined criterion of iterative convergence is achieved.

3. Calculation example

Basic assumptions

The subject of analysis is a three-span beam with a total span 70 m. The beam supports a structural floor above an underground car park. A double-T cross section profile was assumed (markings as per Fig. 5).

The following material and geometrical assumptions were adopted:

- Concrete grade: C50/60
- Prestressing steel Y1770S7
- Geometrical dimensions of the section in relation to height: $h_{f1} = 0.18h$

- $h_{f1} = 0.15h$
- $b_{f1} = 0.43h$
- $b_{f1} = 0.53h$

- Support area width: 2 m
- Maximum tendon channel diameter: 80 mm.
- Minimum axial distance of tendons from the section edge: $a_1 = a_2 = 200$ mm

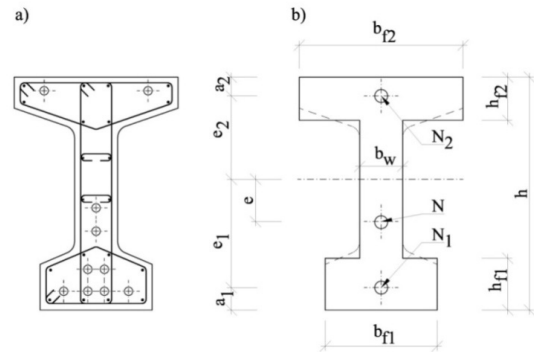


Fig. 5. Section: a) actual, b) calculated

For the prestressed tendon liners required, the web width was designed to be $b_w = 250$ mm. In addition to that, the 200 mm limits on the minimum dimensions of shelves were introduced.

The beam is a repeatable component and it supports a precast structural floor made of prestressed slabs. The spacing between girders was set to 8 m. The maximum allowable beam height: $h_{max} = 2.1$ m.

- The overall fixed load assumed: 5.4 kN/m².
- The operational load assumed: 5.0 kN/m².
- The long-term part of variable load coefficient assumed was $\psi = 0.6$.

For the consequences of component damage, no formation of cracks is allowed (yet, tensile stress is acceptable that does not exceed the tensile strength of concrete). In addition to that the compressive stress limit $0.6f_{ck}$ was introduced for concrete, both for the initial and fixed conditions.

Since, in the optimisation task, limitations were imposed on the maximum compressive and tensile stress, the method of allowable stress was adopted in calculations for safety evaluation (the limit condition method was abandoned). The method consists in calculating the normal stress σ in the structural material, and then comparing it to the allowable stress.

Loading phases and computational combinations

Figure 6 below shows the loading phases:

- Phase_I - loading with own weight g_{cw} and fixed load $g_{1, 2, 3}$;
- Phase_{II, III, IV, V, VI} - various operating load configurations;
- ΣN - compression.

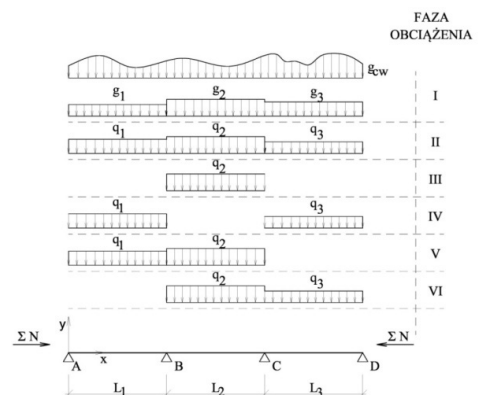


Fig. 6. Loading phases

Phase I was additionally divided into two parts: loading with the own weight and fixed load. This division aims to create a computational combination for the initial condition of the component performance.

In the general optimisation task, the fixed and operating load was assumed with a constant value, but varying for individual beam spans. Given the possibility of cross sectional variation in the general optimisation task, the own weight of the component is described with a non-linear function. In the task analysed $g_1 = g_2 = g_3$ and $q_1 = q_2 = q_3$ was assumed.

The beam analysed remains in the assumed loading condition. Table 2 summarises the possible computational combinations of fixed operating loads and the prestressing load in the permanent condition. Additionally, the K0 combination of the initial condition was created (own weight loading and the effect of prestressing, without external load).

Tab. 2. Computational combinations in permanent condition

Loading phases	Computational combinations					
	K1	K2	K3	K4	K5	K6
F _I	X	X	X	X	X	X
F _{II}		X				
F _{III}			X			
F _{IV}				X		
F _V					X	
F _{VI}						X
Σ N	X	X	X	X	X	X

In the solution, any configuration of the possible prestressing tendon routes is allowed (according to Table 3). With the above assumptions, the task is not limited to determine the optimum resultant tendon route only, but also to finding an optimum method for prestressing the component given as well.

Tab. 3. Possible combinations of prestressing tendon trajectories

Tendon	Resultant tendon		
	N	N ₁	N ₂
N _I	X		
N _{II}		X	
N _{III}			X
N _{IV}	X	X	X
N _V	X	X	
N _{VI}	X		X
N _{VII}		X	X

According to the above tables, the overall number of computational combinations is:

$$\sum K_i \sum N_j = 49 \tag{17}$$

Calculation results

1st iteration

While minimising the concrete volume, the objective function is not the prestressing force. Therefore, in the calculations, the prestressing force was not determined before considering the prestressing loss. All the values specified determine the force after all present and delayed loss. In order to reach an accurate solution, the original prestressing force before the loss should be specified. However, due to the objective function assumed for the optimum solution, no prestressing force values before loss was specified.

The minimum section height obtained in the preliminary calculations was $h = 1.60$ m. This value was obtained for 108 possible routes of the resultant tendon. The variability range of the overall prestressing force was $(8000 \div 11000)$ kN.

Optimum solutions were selected those which, apart from minimising the height h , showed the lowest value of the

prestressing force (a total of 21 from 108). The solution for the total prestressing force is shown below, which is 8000 kN ($N = 3000$ kN, $N_1 = 2000$, $N_2 = 3000$ kN).

The figures showing the prestressing tendon routes also specify the locations of the characteristic points. For all figures showing the prestressing location, the vertical axis range corresponds to the beam height. In figures depicting the boundaries of normal stress, the limit values, adopted as the optimisation criteria, are also shown.

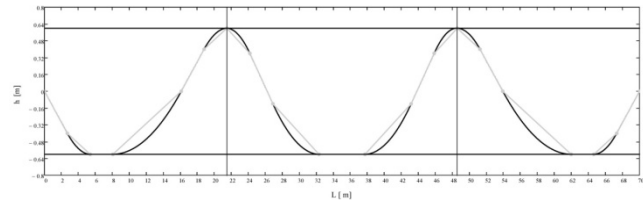


Fig. 7. Prestressing tendon routes (preliminary calculations)

1st iteration

Calculations of the 1st iteration were based on the following assumptions:

- division of section L_1 to 11 characteristic ranges;
- division of section $0.5 L_2$ to 7 characteristic ranges;
- height variability $h: <1.55 ; 1.60>$, m;
- variability of the prestressing force $N: <2000 ; 4000>$, kN;
- variability of the prestressing force $N_1: <1000 ; 3000>$, kN;
- variability of the prestressing force $N_2: <1000 ; 4000>$, kN;
- increment $\Delta h = 0.05$ m;
- increment $\Delta N = \Delta N_1 = \Delta N_2 = 1000$ kN.

As a result of dividing the section L_1 into 11 parts, the characteristic range with the length 1.950 m was obtained, and by dividing the section $0.5L_2$ into 7 parts, the range of 1.936 m is obtained. The configuration of characteristic ranges provided results in 64,680 possible configurations of the coordinates X characteristic points of the route. Due to a great number of the possible locations of the resultant tendon route in the first iteration, the range h assumed was: $<1.55 ; 1.60>$, m. Given the division $n_y = 4$ the size of the base XYh was 64,680. Calculations of the first iteration are aimed at eliminating the prestressing tendon routes for which it is impossible to meet the optimisation limitations.

Considering the large data set, the size of finite elements adopted was consistent with the size of the characteristic ranges. The division assumed resulted in obtaining overall 36 finite elements (for the entire beam length). The above accuracy of FEM is sufficient to obtain results which are accurate enough, without the risk of potentially corrects solutions being rejected, while ensuring fast numerical calculations.

Because of the variability of the prestressing forces, 23,284,800 different height configurations were considered in the calculations, for the resultant tendon height and prestressing forces.

The solution is shown below for $h = 1.55$ m and the total prestressing force is shown which is 8000 kN ($N = 3000$ kN, $N_1 = 2000$, $N_2 = 3000$ kN). The figures present the prestressing tendon routes, inner force boundaries, inner forces caused by prestressing, boundaries of nodal displacements and normal stress for one selected solution meeting the optimisation criteria.

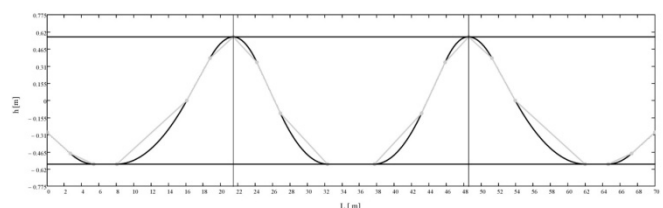


Fig. 8. Prestressing tendon route (first iteration)

2nd iteration

Since for calculations the result base from the first iteration was used, a considerably smaller data set was available. Therefore, the division of the section L_1 to 22 finite elements and the section $0.5L_2$ to 14 elements was assumed. As a result of the division adopted, overall 72 finite elements were obtained (for the entire beam length), with the length respectively 0.975 m (for section L_1 and L_3) and 0.968 m (for section L_2).

Calculations of the 2nd iteration were based on the following assumptions:

- height variability h : $\langle 1.45 ; 1.55 \rangle$, m;
- variability of the prestressing force N : $\langle 2500 ; 3500 \rangle$, kN;
- variability of the prestressing force N_1 : $\langle 1000 ; 2000 \rangle$, kN;
- variability of the prestressing force N_2 : $\langle 2000 ; 3500 \rangle$, kN;
- increment $\Delta h = 0.01$ m;
- increment $\Delta N = \Delta N_1 = \Delta N_2 = 250$ kN.

The calculations resulted in a series of solutions with the minimum value $h = 1.47$ m, while the variability range of the overall prestressing force was (7500 – 9250) kN. The figures below summarise the results for one chosen possible solution with the lowest overall prestressing force value of: 7500 kN ($N = 3000$ kN, $N_1 = 1500$, $N_2 = 3000$ kN).

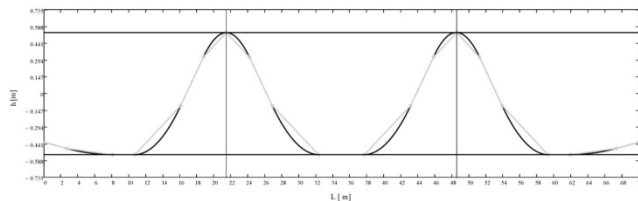


Fig. 9. Prestressing tendon route (second iteration)

Following iterations

In the third iteration the characteristic ranges were densified. For calculations, the result base of the second iteration was adopted, from which the results for which the height $h > 1.47$ m had been removed. As a result of the densification, the characteristic range X reduced the lengths to 0.975 m for L_1 and 0.968 m for L_2 . The length not exceeding 1 m is a very precise value that makes it possible to obtain an accurate result. In practice (for technical reasons), curvilinear sections measuring less than 1 m are rarely used.

In the fourth iteration, the characteristic ranges were not densified, but the accuracy of prestressing forces was increased. Finally, for the fourth iteration: $\Delta N = \Delta N_1 = \Delta N_2 = 50$ kN. Moreover, the division n_y was increased to 10. Increment $\Delta h = 0.1$ m.

The calculations were interrupted after the fourth iteration. The optimum solution is presented below.

- $h = 1.43$ m
- $N = 2950$ kN
- $N_1 = 1450$ kN
- $N_2 = 3150$ kN

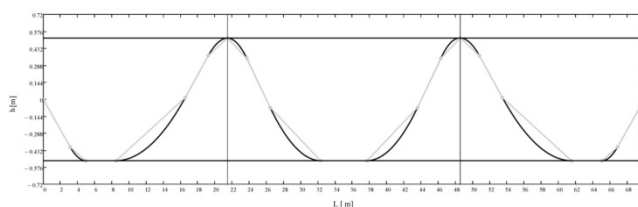


Fig. 9. Prestressing tendon route (final results)

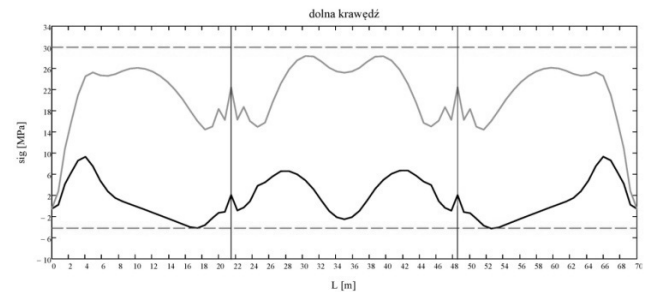


Fig. 10. Boundary of normal stress - lower edge (final results)

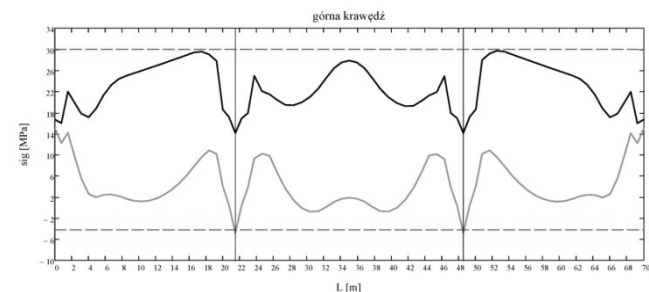


Fig. 11. Boundary of normal stress - upper edge (final results)

4. Conclusions

The article gives a brief overview of the original optimisation method being developed. Innovative design method is presented that allows quick finding of optimum solutions. Combined with a FEM algorithm, the method provides vast opportunities contemporary design. Due to relatively short time required, the method can be utilised by offices designing building structures to optimise various components and even entire construction systems. The optimisation task can be formulated in any programming language or with the aid of common mathematical software.

According to the analyses performed, a correctly assumed prestressing is of key importance for optimum forming of post-tensioned concrete components. Designing post-tensioned concrete components should not be limited to only one resultant tendon route. However, in design practice, usually only one resultant prestressing tendon is considered. Furthermore, the resultant tendon route is usually formed with second order polynomials and is curvilinear over the entire beam length. With the above assumptions, designers tend to create components which differ from the possible optimum solution.

Analysing test results obtained, it was possible to formulate practical recommendations for optimum setting of the prestressing tendon routes, as listed below.

- It is recommended to introduce straight sections of prestressing tendon routes (at the bottom edges), near the centres of inter-span distances at the areas of the extreme bending moments.
- In addition to a variable-trajectory tendon, the benefits from using straight tendons at the upper and lower edge of the cross section should be analysed.

The calculation method presented allows finding quickly a solution to diverse optimisation issues, provided that the calculations are preceded by an in-depth analysis of the task. With the preliminary analysis, it is possible to correctly formulate the problem and reject the solutions which, as a rule do not meet the specified optimisation criteria. Correct determination of the range of decision variables significantly accelerates the calculations and delivers a more accurate outcome.

It is worth mentioning that the gradient iterative method is not limited only to the structure optimisation tasks, but can also be used for finding solutions to other problems.

5. References

- [1] Ajdukiewicz A., Mames J.: Konstrukcje z betonu sprężonego. Polski Cement, Kraków 2004.
- [2] Kluz T. et al.: Wykonywanie betonów sprężonych. Poradnik. Arkady, Warsaw 1965.
- [3] Machelski Cz.: Modelowanie konstrukcji sprężonych. Dolnośląskie Wydawnictwo Edukacyjne, Wrocław 2010.
- [4] Podstawy projektowania konstrukcji żelbetonowych i sprężonych według Eurokodu 2. Praca zbiorowa. Dolnośląskie Wyd. Naukowe, Wrocław 2002.
- [5] Trochymiak W.: Mosty betonowe z naprężanymi cięgnami - ewolucja form konstrukcyjnych i zasad obliczania. Wyd. OWPW, Warsaw 2012.
- [6] Fenner R. T.: Finite Element Methods for engineers. 1997.
- [7] Łodygowski T., Kąkol W.: Metoda elementów skończonych w wybranych zagadnieniach mechaniki konstrukcji inżynierskich. Wydawnictwo Politechniki Poznańskiej, Poznań 1994.
- [8] Rakowski G., Kacprzyk Z.: Metoda elementów skończonych w mechanice konstrukcji. Oficyna Wyd. Pol. Warsz., Warsaw 2005.
- [9] Sobczyk Sz.: Optymalne kształtowanie pólek dźwigarów strunobetonowych. Badania doświadczalne i teoretyczne w budownictwie. monografia. Wyd. Pol. Śląskiej, Gliwice 2012.
- [10] Sobczyk Sz., Mikulski L.: Zastosowanie gradientowo-iteracyjnej metody optymalizacji na przykładzie belki wspornikowej. Pomiary Automatyka Kontrola no. 11/2013. Wyd. PAK, Gliwice; 2013.
- [11] PN-EN 1990:2004: Basic design rules of structures.
- [12] PN-EN 1991-1-1:2004: Actions on structures - General actions - Densities, self-weight, imposed loads for buildings.
- [13] PN-EN 1992-1-1:2008: Design of concrete structures - General rules and rules for buildings.

[14] PN-EN 1992-1-2:2008: Design of concrete structures - General rules - Structural fire design.

Received: 15.01.2016

Paper reviewed

Accepted: 02.03.2016

Szymon SOBCZYK, PhD, eng.

Designer of building structures. Research and teaching assistant professor at the Department of the Fundamentals of the Mechanics of Continuous Media Krakow University of Technology. Graduate from the AHG University of Science and Technology in Krakow (major in: geodesy and cartography) and from Krakow University of Technology (major in: civil engineering). Research and scientific interests in the field of optimum forming of structures.

e-mail: szymek.sobczyk@gmail.com



Prof. Leszek MIKULSKI, PhD, eng.

Student's Affairs Deputy Chancellor and Head of the Department of Fundamentals of the Mechanics of Continuous Media, Faculty of Civil Engineering Krakow University of Technology. Research and scientific interests in the field of optimum forming of structures and systems, author of 50 publications on this subject.

e-mail: ps@pk.edu.pl

